Journal Pre-proof

Integrated network pharmacology and zebrafish model to investigate dual-effects components of *Cistanche tubulosa* for treating both Osteoporosis and Alzheimer's Disease

Ying-Qi Li, Yi Chen, Jia-Yi Fang, Si-Qi Jiang, Ping Li, Fei Li

PII: S0378-8741(19)34540-4

DOI: https://doi.org/10.1016/j.jep.2020.112764

Reference: JEP 112764

To appear in: *Journal of Ethnopharmacology*

Received Date: 15 November 2019

Revised Date: 2 March 2020

Accepted Date: 10 March 2020

Please cite this article as: Li, Y.-Q., Chen, Y., Fang, J.-Y., Jiang, S.-Q., Li, P., Li, F., Integrated network pharmacology and zebrafish model to investigate dual-effects components of *Cistanche tubulosa* for treating both Osteoporosis and Alzheimer's Disease, *Journal of Ethnopharmacology* (2020), doi: https://doi.org/10.1016/j.jep.2020.112764.

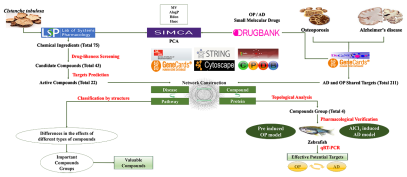

Integrated network pharmacology and zebrafish model to investigate dual-effects components of *Cistanche tubulosa* for treating both Osteoporosis and Alzheimer's Disease

Ying-Qi Li [1], Yi Chen [1], Jia-Yi Fang [1], Si-Qi Jiang [1], Ping Li [1, *] and Fei Li [1, 2, *]

[1] State Key Laboratory of Natural Medicines, China Pharmaceutical University, Nanjing 210009, China; lifeicpu@163.com

[2] College of Pharmacy, Xinjiang Medical University, Urumqi 830011, China; lifeicpu@163.com

[*] Correspondence: lifeicpu@163.com (F.L.); liping2004@126.com (P.L.); Tel.: + 86 25 8327 1382

ABSTRACT

Ethnopharmacological relevance: Osteoporosis (OP) and Alzheimer's disease (AD) are common geriatric concurrent diseases, and many studies indicate the connection of their pathogenesis. *Cistanche tubulosa* (Schenk) Wight (CT) is a widely used traditional Chinese medicine and has been extensively applied to treat OP and AD, respectively. However, the active ingredients for both concurrent diseases simultaneously and underlying mechanisms are limited.

Aim of study: This work aimed at establishing an effective and reliable network screening method to find dual-effects compounds in CT that can protect AD and OP concurrently. And it will provide new perspectives of the link between OP and AD on molecular mechanisms.

Material and methods: The dual-effects of CT were systematically analyzed with integrating multiple databases and extensive analysis at a network pharmacology level. Classified drug-target interaction network was constructed to reveal differences in effects between different types of compounds. To prove the effectiveness of this

network, some compounds were selected to verify in Pre-induced OP model and $AlCl_3$-induced AD model of zebrafish according to the topological parameters.

Results: 22 dual-effects active ingredients in CT were initially screened out via network pharmacology with a closely connection with 81 OP and AD-related targets. Classified network analysis found the better bioactivities of phenylethanoid glycosides and flavonoids. The dual-effects of four selected compounds demonstrated that the network is reasonable and effective, suggesting the dual-effects of the remaining 18 compounds. Moreover, we identified 9 putative targets and two pathways that were significantly related to OP and AD.

Conclusions: We successfully identified 22 dual-effects active components in CT. This systematic screening strategy provided a new protocol to objectively discover multi-effects compounds of traditional Chinese medicine, and even a macroscopic perspective that will improve our understanding of the link between OP and AD on molecular mechanisms.

Keywords: Network Pharmacology; Osteoporosis; Alzheimer's disease; *Cistanche tubulosa*; Zebrafish.

1. Introduction

Aged tendency of population results in the increased prevalence of osteoporosis (OP) and Alzheimer's disease (AD) by years (Parnetti et al., 2019; Rizzoli, 2018). Nowadays both OP and AD have been recognized as major threats for public health since they may progress without symptoms and bring huge social burden (Erkkinen et al., 2018; Jonsson et al., 2018). As age-related diseases, they are often seen to

co-occur in clinical practice with a high disability and fatality rate (Dengler-Crish and Elefteriou, 2019). OP is a systemic skeletal disease characterized by low bone mass and impaired micro-architecture of bone tissue, with enhanced bone fragility and increasing risk of fractures (Rizzoli, 2018). AD is the most common brain degeneration characterized by progressive loss of memory and other cognitive functions (Bondi et al., 2017). Until now, there are still no sufficiently powerful options to prevent, or cure the two diseases since their complex etiology and pathogenesis. And what's worse is that the patient is more often to side effects (Brown, 2017; Huang and Mucke, 2012).

On the theoretical basis of syndrome differentiation (Sucher, 2013), traditional Chinese medicines (TCMs) with multiple components targeting more than one pathophysiological mechanism have a unique superiority in the treatment of some familiar complex diseases. As a kidney tonic herb, *Cistanche tubulosa* (Schenk) Wight (CT) is widely used to against memory loss and atrophic debility of bones by traditional Chinese physicians (Fu et al., 2018). Beside its traditional efficacy, considerable researches showed that it had various pharmacological activities, such as ameliorating the cognitive and behavioural deficits (Wu et al., 2014), anti-inflammatory (Fu et al., 2018), promoting bone formation and suppressing bone resorption (Li et al., 2013; Li et al., 2012), as well as antioxidant activity (Zhang et al., 2016). But the complicacy of its active ingredients and metabolic process raised difficulties on both exploring targets in human tissues and expounding the mechanism of action.

Above all, a reliable discussion of the therapeutic targets of OP/AD is necessary. Especially basing on the thought of "same treatment for different diseases" in TCMs, and the methodologies of "multi-component therapeutics, biological network" in network pharmacology, the attempts to search for significative common-targets between both diseases may have a particularly practical meaning in providing guidance for the prevention and control of OP and AD.

Zebrafish have strong similarities in their skeletal physiology to mammals and highly homologous genes to human. It's an available and attractive animal model in *vivo* for OP and AD research (Bergen et al., 2019; Newman et al., 2014). Thus, this network pharmacology research was aimed at screening dual-effects active constituents of CT, exploring the common potential targets of OP and AD, as well as to uncover the possibility of using CT to treat two diseases concurrently. In this study, the targets' information of CT active ingredients, genomes and proteomics information of OP and AD were respectively collected from different databases to establish an interactive network, and enrichment analysis was constructed to discover synergistic mechanisms of CT for treating OP and AD. Furthermore, we induced OP and AD zebrafish model respectively and captured the key compounds in the network to verify their efficacy and targets on two diseases.

2. Materials and methods

2.1 Reagents

Chemical standards of genistein (GE), quercetin (QU), abietic acid (AA), β-sitosterol (BSS) (purity $\geqslant$ 98%) were purchased from Chroma Biotechnology Co., Ltd.

(Chengdu, China). Culture plates were obtained from Wuxi NEST Biotechnology Co., Ltd. (Wuxi, China). Prednisolone (Pre), Etidronate Disodium (Ed), Donepezil HCL (DPZ), $AlCl_3 \cdot 6H_2O$ was purchased from Aladdin Reagent Inc. Zebrafish alkaline phosphatase (ALP), tartrate resistant acid phosphatase (TRAP), acetylcholinesterase (AChE), and choline acetyltransferase (ChAT) enzyme-linked immunosorbent assay (ELISA) kit were supplied by Shanghai Enzyme-linked Biotechnology Co., Ltd. (Shanghai, China). Trizol was obtained from Nanjing KeyGen Biotech. Co., Ltd. (Nanjing, China). TransStart Top Green qPCR SuperMix was purchased from TransGen Biotech. Co., Ltd. (Beijing, China).

2.2 Animals

Adult zebrafish (AB strain, 4 months old) were maintained at 28°C under 14/10 h light/dark cycle in an aquarium supplied with fresh water exchange. They were kept two times daily with newly-hatched brine shrimp diet (Chen et al., 2018). Normally fertilized embryos were selected and cultured to 3 days post-fertilization (dpf) in a light growth incubator. All animal experiments were in accordance with the guidelines of the institution and government for animal experiments.

2.3 Network Pharmacological Process

2.3.1 Chemical Space Calculation and Candidate Compounds Screening

All the chemical ingredients data of CT were collected from Traditional Chinese Medicine Systems Pharmacology Database and Analysis Platform (TCMSP, http://tcmspw.com/). TCMSP is a systems pharmacology platform of Chinese herbal medicines that captures the relationships between drugs, targets, and diseases (Ru et

al., 2014). Meanwhile, four essential pharmacology-related parameters in TCMSP were acquired for the principal component analysis (PCA), including molecular weight (MW), partition coefficient between octanol and water (AlogP), hydrogen donor count (Hdon) and hydrogen acceptor count (Hacc). The chemical distribution of CT was built with the above parameters using the SIMCA software (Version 14.1, Umetrics). And small molecule drugs approved for AD/OP from DrugBank (https://www.drugbank.ca/) were processed in the same course.

Ingredients from CT were filtered by drug-likeness (DL). DL is a qualitative concept used in drug design for an estimate on how "drug-like" a prospective compound is. This vital property is used as a selection criterion for the "drug-like" compounds in the traditional Chinese herbs and it helps to optimize pharmacokinetic and pharmaceutical properties (Tao et al., 2013). Based on suggestions in literatures and TCMSP, we selected DL $\geq$ 0.18 as filter conditions. The ingredients conforming to the condition were exported for subsequent analysis. Their 2-dimensional (2D) and 3D structures were painted by ChemDraw Professional 16.0 software. And the 3D structures were optimized by the function of minimizing energy in Chem3D 16.0.

2.3.2 OP and AD Associated Targets Collection

All gene associations for OP and AD were independently collected from DisGeNET (http://www.disgenet.org/web/DisGeNET) and GeneCards. The DisGeNET database is one of the largest publicly available discovery platform of genes and variants associated with human diseases (Pinero et al., 2017). GeneCards (https://www.genecards.org) is an integrated database of human genes that including

genomic, transcriptomic, proteomic, genetic, clinical and functional information (Safran et al., 2010).

2.3.3 Compound Targets Collection and Inverse Docking Prediction

GeneCards database and Swiss TargetPrediction database were combined to predict relevant targets of active ingredients in CT. GeneCards indicates the known active targets of compounds, whereas Swiss TargetPrediction database (http://www.swisstargetprediction.ch/index.php) can estimate the most probable macromolecular targets of small molecules (Daina et al., 2019). Before prediction, the structures of candidate molecules were converted from mol2 format to SMILES format by using Open Babel (Version 2.4.1).

2.3.4 Protein-protein Interaction Analysis

STRING database (https://string-db.org/) was applied to discover the interactions among a group of CT-OP-AD shared targets. After searched under the pattern of "Homo sapiens", the protein-protein interaction (PPI) network was visualized by Cytoscape (Version 3.7.2) software. STRING is a database of known and predicted PPI, derived from genomic context predictions, high-throughput lab experiments, (conserved) co-expression, automated textmining and previous knowledge in databases (Szklarczyk et al., 2017).

2.3.5 GO and KEGG Pathway Enrichment Analysis

Gene Ontology (GO) enrichment analysis was performed on Funrich software (http://www.funrich.org/). FunRich (Version 3.1.3) is a functional software used mainly for enrichment analysis of genes and proteins (Pathan et al., 2015).

ConsensusPathDB-human database (CPDB, http://cpdb.molgen.mpg.de/) was employed to conduct the pathway enrichment analysis. The obtained gene list was submitted to the database with setting "p-value cutoff" as 0.01. After getting the results, only these pathways related to OP and/or AD were selected and divided into groups according to KEGG function categories (https://www.kegg.jp/kegg/pathway.html). CPDB is a seamless interaction network containing binary and complex protein-protein, genetic, metabolic, signaling, gene regulatory and drug-target interactions, as well as biochemical pathways in Homo sapiens (Kamburov et al., 2013).

2.4 Experimental Procedures for OP Zebrafish Model

2.4.1 Model Grouping

Zebrafish larvae were divided into several groups: control group, model group, model + Ed group, model + compounds groups, each of which contained 30 larvae. The control group was maintained in the medium with 0.2% DMSO. The model group was treated with Pre (25 μM) from 3 dpf to 8 dpf. The model + Ed group was co-treated with Pre and Ed (30 μg/mL).

2.4.2 Alizarin Red Staining

After 5 days culture with different compounds, larvae were anesthetized, fixed and bleached in turn. Alizarin red was used to stain the head bones of zebrafish. 1% KOH and glycerol (ratios of 3:1, 1:1 and 1:3) were applied respectively to remove excess. Finally, stereomicroscope (Olympus SZX16) was employed to capture the zebrafish staining images under the prone position. Staining area and integrated optical density

(IOD) were calculated by Image-Pro Plus 6.0.

2.4.3 ALP and TRAP Activity Determination

Zebrafish larvae at 3 dpf were subcultured in 6-well plates and incubated with Pre in the presence or absence of compounds for 5 days. Then they were collected for measuring ALP activity. ALP activity was determined by using the zebrafish ALP ELISA kit based on the manufacturer's protocol. The method to evaluate TRAP activity was same as ALP.

2.5 Experimental Procedures for AD Zebrafish Model

2.5.1 Model Grouping

Zebrafish larvae were divided into several groups: control group, model group, model + DPZ group, model + compounds groups, each of which contained 30 larvae. The control group was maintained in the medium with 0.2% DMSO. The model group was treated with $AlCl_3$ (150 μM, pH 5.8) from 3 dpf to 6 dpf. The model + DPZ group was co-treated with $AlCl_3$ and DPZ (8 μM).

2.5.2 Behavioral Analysis

After 3 days drug deliveries, larvae movement was recorded by ViewPoint behavior analyzer (Zebralab 2018, ViewPoint Life Sciences Co., Ltd.). All experiments were completed in 60 min at 28˚C, containing 3 cycles of light/dark phase (10 min each for light and dark). According to the methods in the previous report, average speed (AS), speed change (ΔS), dyskinesia recovery rate (DRR, equation a) and response efficiency (RE, equation b) are selected as the anti-AD drug efficiency evaluation index in this model (Pan et al., 2019; Wenhai et al., 2016).

$$AS\ (\text{mm/sec}) = D / T,\ DRR\ (\%) = 100 \times (AS_{Drug} - AS_{Model}) / (AS_{Control} - AS_{Model}), \quad \text{a}$$

where D is the movement distance of zebrafish during 60 min, T is the experimental time.

$$RE\ (\%) = 100 \times (\Delta S_{Drug} - \Delta S_{Model}) / (\Delta S_{Control} - \Delta S_{Model}), \quad \text{b}$$

where ΔS is the speed change of zebrafish in light/dark cycles.

2.5.3 AChE and ChAT Activity Measurement

Zebrafish larvae at 3 dpf were subcultured in 6-well plates and incubated with $AlCl_3$ in the presence or absence of compounds for 3 days. Then they were collected for AChE activity. AChE activity was detected by using the zebrafish AChE ELISA kit based on the manufacturer's protocol. The method to evaluate ChAT activity was same as AChE.

2.6 Quantitative Real-Time PCR Analysis

Zebrafish larvae were divided into OP and AD groups. OP groups consisted of control group, Pre group, and Pre + compounds groups, cultured from 3 dpf to 8 dpf. AD groups included control group, $AlCl_3$ group, and $AlCl_3$ + compounds groups, cultured from 3 dpf to 5 dpf. Each group contained 30 larvae. Total RNA was respectively extracted from these zebrafish larvae samples by Trizol. RNA samples were reverse-transcribed to cDNA according to manufacturer's instruction of the cDNA kit. The mRNA expression level was detected by real-time fluorescent quantitative PCR (Roche LightCycler96). The results were normalized to β-actin expression and quantified by the comparative ($2^{-\Delta\Delta Ct}$) method. Forward and reverse primers used were synthesized by Sangon Biotech (Shanghai, China) and listed in Supplementary Table S1.

2.7 Statistical Analysis

GraphPad Prism version 8.00 was used for descriptive statistical analyses. Data were expressed as mean ± SD and analyzed by ANOVA method to test for variability between each trial considering $P \leqslant 0.05$ as significant.

3. Results

3.1 Candidate Compounds and Potential Targets

In the research of CT chemical constituents, a total of 75 ingredients were obtained from TCMSP. Then PCA was conducted to visualize the chemical distribution of CT. As shown in Figure 1, the ingredients of CT were multifarious in chemical space, and 28 of them satisfied the Lipinski's rule of five (Lipinski, 2003). Interestingly, there were many overlapping parts between the ingredients of CT and approved small molecule drugs for OP/AD. It illustrated that many compounds in CT had the potential druggability on OP/AD. To further evaluate their druggability, 43 compounds were screened by DL. After targets prediction, 26 candidate compounds were selected for the subsequent analysis. And they can be docked with a total of 847 target proteins.

The gene entries related to OP or AD were collected from the DisGeNET and GeneCards databases. As a result, 3052 and 8042 gene entries were respectively collected. We adopted the two scores from the DisGeNET and GeneCards databases as evaluation score, screening the top fifth of targets. The one-fifth ratio was decided by pre-experiments. Then 211 OP-AD common targets were preserved to match with the targets of 26 candidate compounds. Finally, total 81 protein targets (Supplementary Table S2) connecting with 22 candidate compounds (Supplementary Table S3) were selected for molecular mechanisms of action analysis, forming a protein-protein interaction (PPI) network shown in Figure 2.

The 22 compounds were divided into 11 categories: 5 phenylethanoid glycosides (PhGs) (Decaffeoylacteoside, Cistanoside E, etc.), 3 phenylacryl oligosaccharides

(Cistanoside H, Cistanoside F, etc.), 3 iridoids and iridoid glycosides (Leonuride, Geniposidic acid, etc.), 3 lignans and lignan glycosides (Yangambin, (+)-Pinoresinol-O-β-D-glucopyranoside, etc.), 2 flavonoids (quercetin, genistein), 1 alkaloid, 1 terpene, 1 sterol, 1 fatty alcohol, 1 fatty acid, and other. According to previous reports, these compounds are the main components or active functional ingredients of CT (Fu et al., 2018).

In Figure 2, a total of 81 common targets were found to have correlations with OP and AD. The degree of PPI was adopted as a characteristic parameter to define the significance of potential targets. Top 5 putative target proteins associated with OP and AD were albumin (ALB), insulin (INS), interleukin 6 (IL6), TNF-alpha (TNF), and epidermal growth factor (EGF).

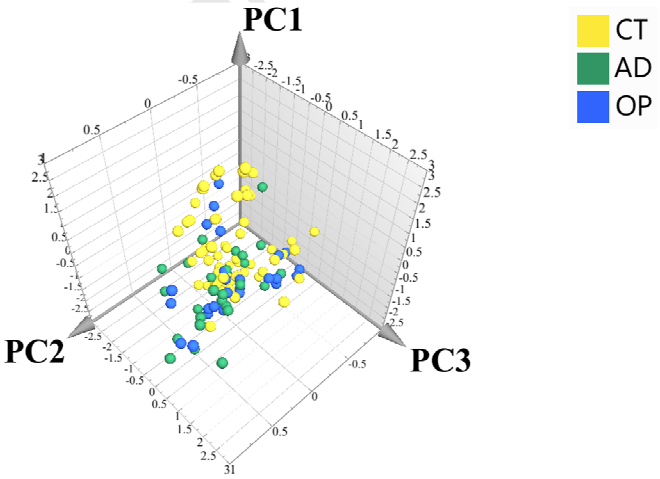

Figure 1. Chemical distribution based on principal component analysis (PCA). PC1, PC2, and PC3 account for 0.654, 0.112, and 0.219, respectively.

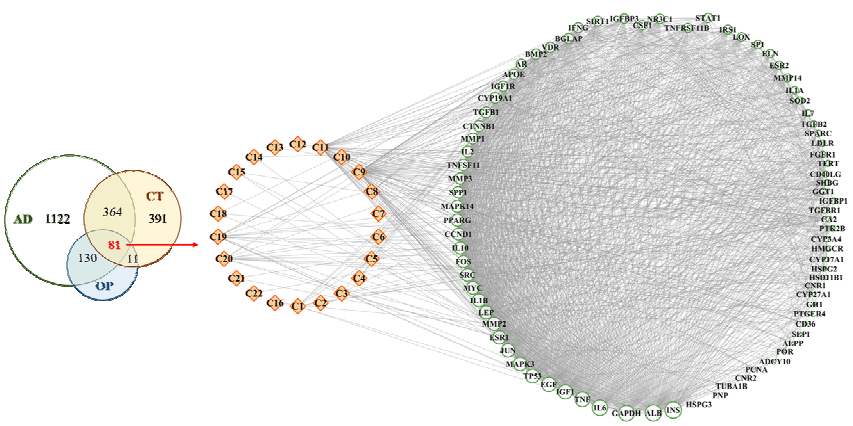

Figure 2. The number of CT, OP and AD targets prediction and the Compound-Target network of CT. White nodes with green edges are the OP-AD shared targets. Orange nodes are active ingredients of CT interacted with the shared targets. The size of nodes reflects the degree of PPI.

3.2 Integrated and Classified Network Analysis

81 putative target proteins in Table S2 were selected to initiate GO and KEGG pathway enrichment analysis. After filtering by *p*-value (GO cut-off of ≤ 0.05, KEGG pathway cut-off of ≤ 0.01), 15 GO terms and 66 KEGG pathway terms were returned, as shown in Figures 3 and 4. A total of 16 GO terms are included: 5 for molecular function, 5 for biological processes, and 6 for cellular component. Since this study was aimed to discover the potential common pathogenesis of OP and AD, we removed the pathway terms directly related to other diseases and classified the rest into different functional categories. It suggested that the 22 active ingredients of CT might regulate a total of 66 pathways which mainly correlated with signal transduction, endocrine system, immune system, cell growth and death to play a confrontational role against OP and AD.

To reveal the differences in the action of different types of compounds, the PPI network constructed in Figure 2 was analyzed according to their categories in Table S3. Figure 5 illustrated that 5 PhGs, 2 flavonoids, 1 terpene, and 1 sterol, particularly flavonoids, might be more important than other ingredients of CT against OP and AD. After that, these 4 series of active compounds were chosen to uncover their compressed pathways. As can be seen from Figure 6, PhGs, flavonoids, terpene, and sterol worked together or alone on 27 pathways, containing 11 modules: cell growth and death, endocrine system, immune system, signal transduction, development, and others. Results suggested that these compounds might play a synergistic role in the positive effects of CT on OP and AD. It's worth noting that the protective effects of PhGs could be more remarkable than flavonoids in neurodegenerative disease since PhGs had direct interactions with Alzheimer disease pathway whereas flavonoids were related to signaling molecules and

interaction. Only sterol and terpene were related with lipid metabolism and excretory system. In addition, PhGs, terpene, and flavonoids showed a potential relation with endocrine and metabolic disease.

According to the PPI illustration, 2 flavonoids (GE, QU), 1 terpene (AA), and 1 sterol (BSS) were adopted as the valuable compounds for further research on molecular mechanisms. Interestingly, we found that they all interrelated with MAPK signaling pathway and TGF-beta signaling pathway. And the *p*-value of two pathways also were much higher. Putative targets of 4 valuable compounds and the distribution of their affected proteins in the two pathways were demonstrated in Figure 7.

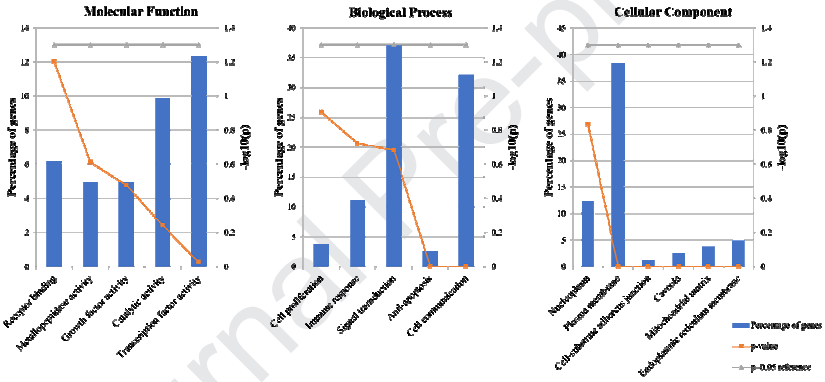

Figure 3. Level2 GO terms enrichment analysis (Molecular Function, Biological Process, Cellular Component).

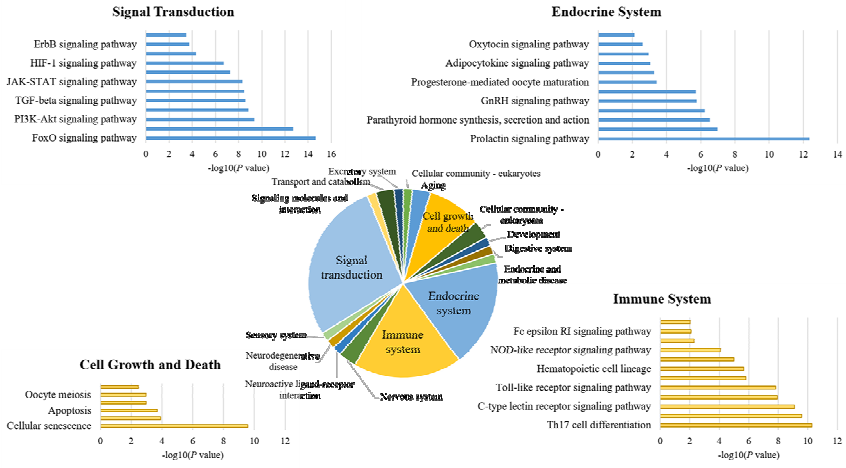

Figure 4. KEGG pathway enrichment analysis.

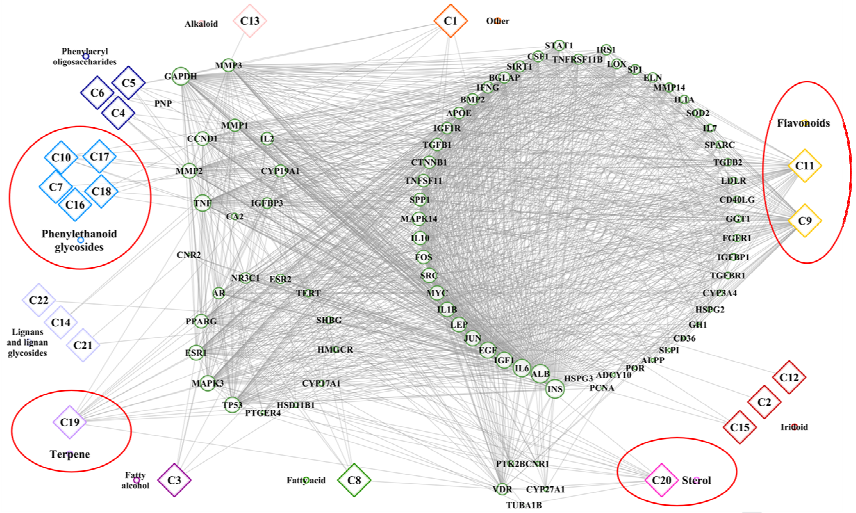

Figure 5. Illustration of Compound-Target network. Rounded nodes with green edges are OP-AD shared targets and the size of nodes reflects the degree of PPI. Diamonds nodes in different colors are the active ingredients of CT grouped by chemical structural types. In this PPI, the four significant compound groups are circled in red.

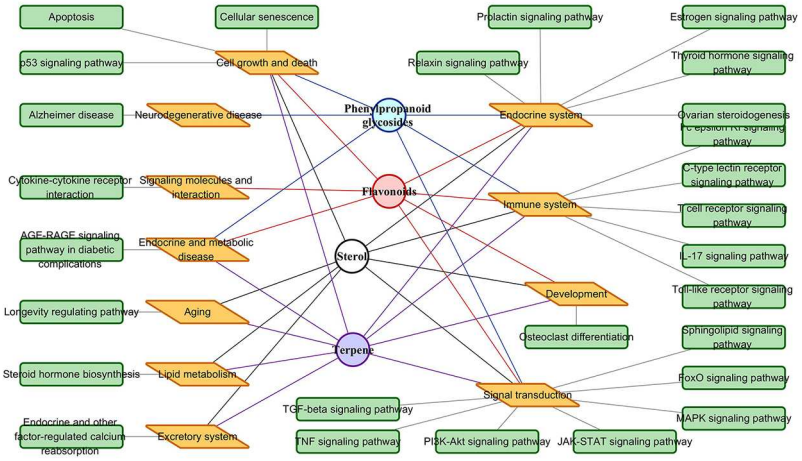

Figure 6. Illustration of KEGG pathway enrichment analysis. Ellipses with different colors are 4 series of valuable ingredients. Parallelograms represents different pathway classifications whereas round rectangles are KEGG pathway terms.

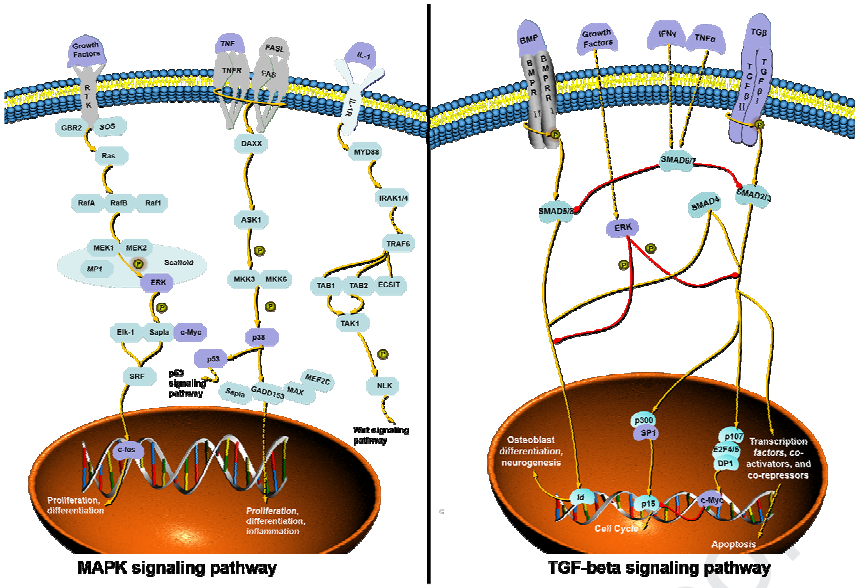

Figure 7. Description of the interactive effects of MAPK and TGF-beta signaling pathway and putative target proteins identified in the present study. Purple targets are related putative target proteins identified in the present study. Yellow lines represent activation whereas red represent inhibition. (Reference: KEGG database).

3.3 Valuable Compounds Efficacy Validation

In this network analysis established in 3.2, we captured 4 valuable compounds for pharmacological activity validation. By the topologically structural analysis method in this study, we found that genistein (GE, C9, DL=0.21), quercetin (QU, C11, DL=0.28), abietic acid (AA, C19, DL=0.28), and β-sitosterol (BSS, C20, DL=0.21) showed feasible interplay to against OP and AD. In this part, zebrafish larvae in vivo models induced by Pre or $AlCl_3$ were established respectively to evaluate the protective effects of 4 compounds against OP and AD.

3.3.1. Effect of 4 compounds on OP

To detect whether 4 compounds have protective effects against OP, Pre was used to establish the OP zebrafish model. The development of osteoblasts was first examined by alizarin red staining to investigate the direct effects of 4 compounds on bone formation. Compared with the control zebrafish, Pre apparently induced a change in bone morphology and bone density of zebrafish skulls in the model group (Figure 8). Declines of staining area and IOD in Pre group and opposite trend in Ed group also

visually demonstrated the success of OP model. What's more, the staining area and IOD of zebrafish skulls in BSS/GE/QU/AA groups were significantly increased compared with the model group (Figure 9). The typical markers of bone formation and resorption such as ALP and TRAP were assayed to further evaluate the anti-osteoporosis effect of 4 compounds. As shown in Figure 10, Pre significantly decreased ALP activity and increased TRAP activity in contrast with the control group. Conversely, Ed and 4 compounds significantly showed the opposite trend to Pre group in the ALP and TRAP activities of zebrafish. These results combined together confirmed that BSS, QU, GE, and AA might play positive roles in bone formation in Pre-induced OP zebrafish.

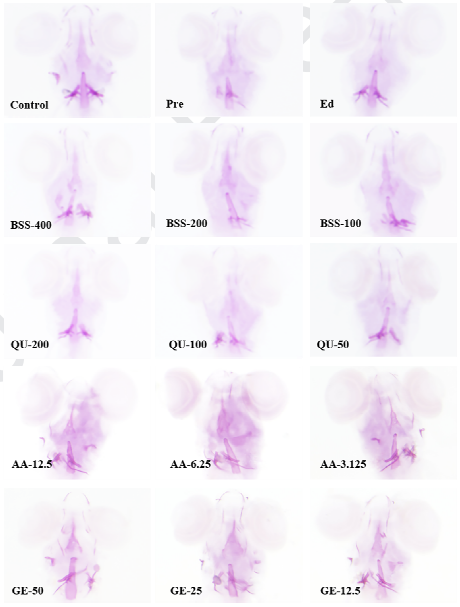

Figure 8. Representative images (100 X) of alizarin red staining in OP zebrafish. 400, 200, 100 μM of BSS, 200, 100, 50 μM of QU, 50, 25, 12.5 μM of GE, and three dosages including 12.5, 6.25, 3.125 μM of AA were used.

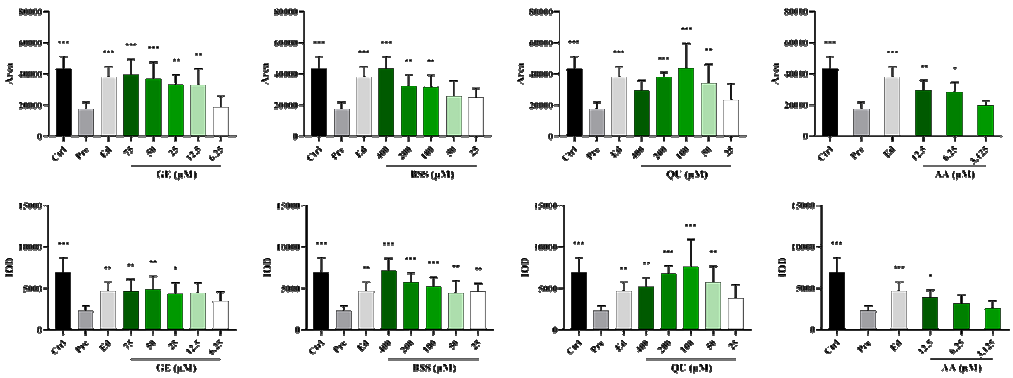

Figure 9. Quantification of alizarin red staining results in OP zebrafish (n=8 per group). Data are mean ± SD, $^{*}P<0.05$, $^{**}P<0.01$, $^{***}P<0.001$, versus Pre group.

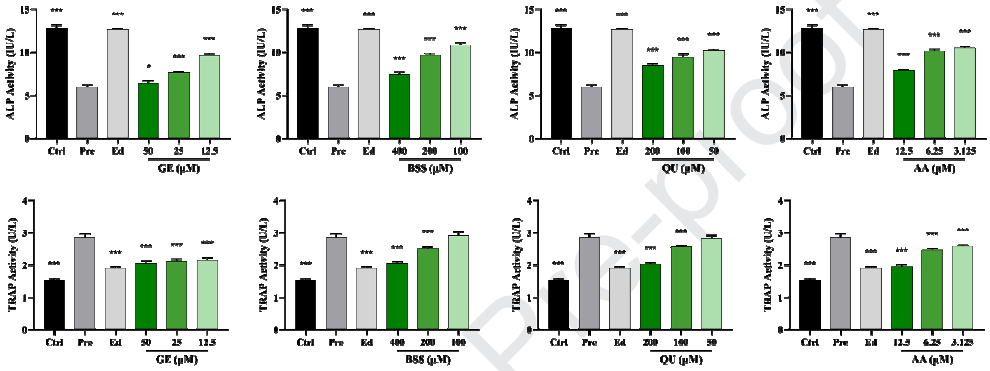

Figure 10. Effect of compounds on ALP and TRAP activity (n = 3). Data are mean ± SD, $^{*}P<0.05$, $^{***}P<0.001$, versus Pre group.

3.3.2. Effect of 4 compounds on AD

To evaluate the protective effects against AD of 4 compounds, the well-recognized $AlCl_3$-induced AD zebrafish model has been used. For this model of AD dyskinesia, the behavior analyzer was used to track the movement of zebrafish. As shown in Figure 11, the AS of $AlCl_3$ group was significantly lower than those of the control group, while for DPZ and all 4 compounds the ASs were close to the control. DRR and RE were listed in Table S4. The results showed that different concentrations of GE, BSS, QU, and AA increased DRR by 2.37-37.64%, 60.18-103.92%, 70.52-164.61%, 2.37-42.64%, respectively with partial significant (p-value < 0.001-0.01). The ΔSs in control group, $AlCl_3$ group and DPZ group further supported that the construction of AD model was successful. RE for GE, BSS, QU, and AA were 13.12-50.45%, 11.41-63.09%, 1.63-66.89%, 13.12-51.09%, respectively. These results with significant differences

demonstrated that GE, BSS, QU, and AA can improve dyskinesia of zebrafish to some extent. Determination of nerve conduction markers (AChE and ChAT) activities in the groups were shown in Figure 12. $AlCl_3$ significantly increased AChE activity and decreased ChAT activity compared with the control group. But DPZ and 4 compounds showed the ability to partial recover the changes caused by $AlCl_3$ in AChE and ChAT activities. It's consistent with the results of rehabilitation effect dyskinesia evaluation. In conclusion, GE, BSS, QU, and AA might have the potential to become prominent anti-AD agents.

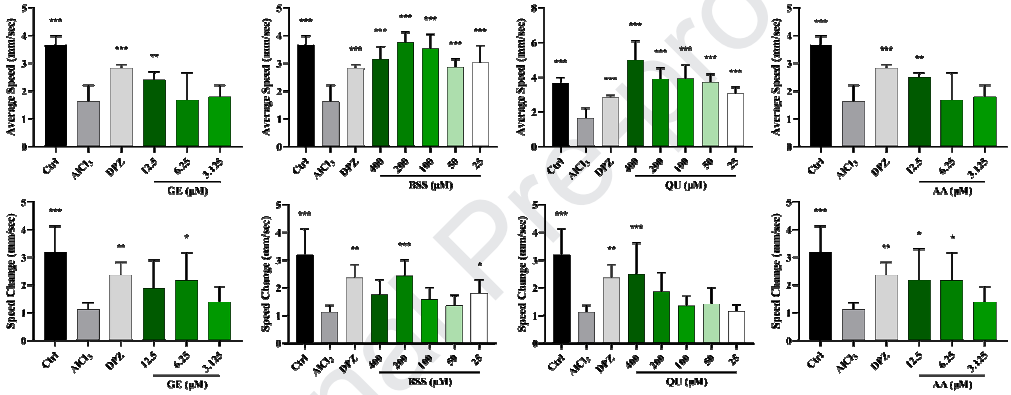

Figure 11. Effect of compounds on behavioral analysis (n = 10). Data are mean ± SD, $^{*}P<0.05$, $^{**}P<0.01$, $^{***}P<0.001$, versus $AlCl_3$ group.

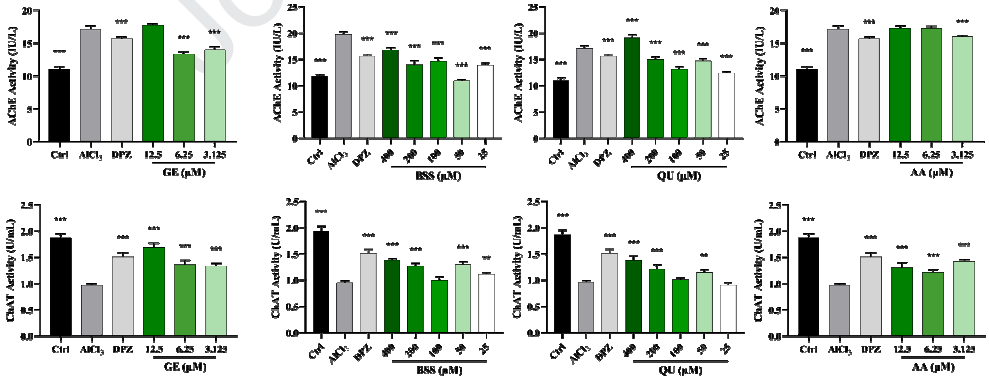

Figure 12. Effect of compounds on AChE and ChAT activity (n = 3). $^{**}P<0.01$, $^{***}P<0.001$, versus $AlCl_3$ group.

3.4 Putative Targets Validation

To verify putative targets which were predicted in this work, targets related to MAPK and TGF-beta signaling pathways were chosen for qRT-PCR analysis. Their relative

mRNA expression levels in the OP model were shown in Figure 13. Compared with the Pre group, GE increased levels of *mapk14a*, *fgfr1b*, *tgfb1*, *bmp2*, and decreased levels of *tp53*, *tnf-α*, *jun*, *tgfbr1*, and *c-fos*. QU increased levels of *mapk14a*, *fgfr1b*, *tgfb1*, *bmp2*, and decreased levels of *tp53*, *jun*, and *il1b*. BSS only showed reducing effects on *tp53*, *tnf-α*, and *mapk3*. As shown in Figure 14, in AD model, GE, QU, BSS, and AA reduced the mRNA expression level of *tp53*. GE and QU both reduced levels of *tnf-α*, *bmp2*, *tgfbr1*, *sp1*, *tgfb2*, and *ifnγ*, and increased level of *jun*, whereas GE and AA increased level of *mapk3*. Only GE appeared to reverse the rise of *mapk14a*, *fgfr1b*, *fgfr1a*, and *igf1ra*. Besides, QU decreased the high levels of *il1b* and *egf*. The relative mRNA expression levels of genes including *tp53*, *tnf-α*, *mapk14a*, *mapk3*, *fgfr1b*, *bmp2*, *jun*, *il1b*, and *tgfbr1* significantly changed by contrast with the control group in each model. These results suggested that they may serve as a link between the two diseases. In addition, these results also suggested the possibility of synergistic effects of 4 compounds.

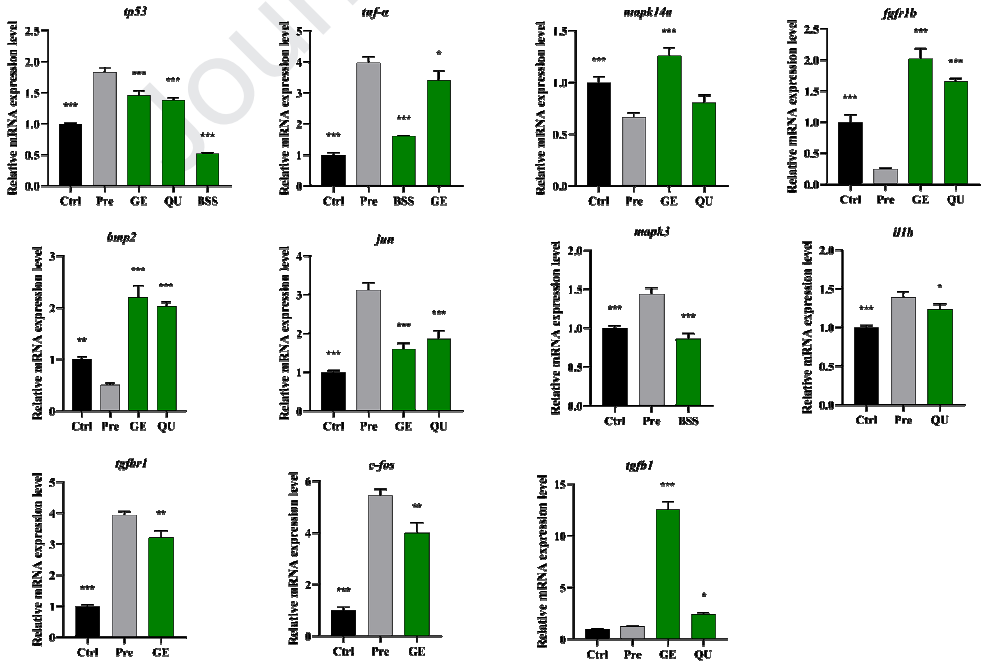

Figure 13. Relative mRNA expression levels in OP zebrafish (n = 3). $^{*}P<0.05$, $^{**}P<0.01$, $^{***}P<0.001$, versus Pre group.

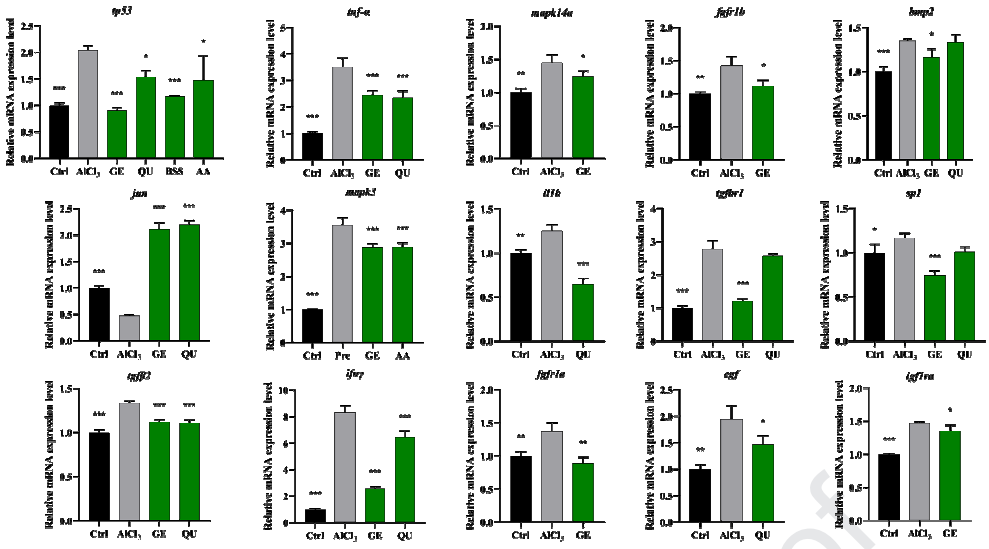

Figure 14. Relative mRNA expression levels in AD zebrafish (n = 3). $^{*}P<0.05$, $^{**}P<0.01$, $^{***}P<0.001$, versus $AlCl_3$ group.

4. Discussion

OP and AD are the most common clinical diseases associated with aging. Their complex pathophysiological mechanisms have limited the effective treatment of two diseases for years. The risk factors of OP and AD demonstrated that the susceptible group of both diseases are partly similar, such as elderly women (Abraham et al., 2013; Patel, 2017), diabetics (Vieira et al., 2018; Xia et al., 2012), long-term smokers (Franic and Verdenik, 2018; Zhong et al., 2015), and inactive individuals (Koedijk et al., 2017; Sofi et al., 2011). Furthermore, current studies have identified that some key proteins in AD also had functions in bone metabolism as well (Li et al., 2016; Pan et al., 2018). There are reasons to believe that OP and AD are not completely independent, even have some potential connections. This suggested a potential homo-therapy for heteropathy, which means treating OP and AD with the same therapy.

On the grounds of the therapeutic objectives and principles of TCM, maladjustment in

a disease can be classified into several “patterns”. So multiple diseases such as OP and AD might share one “pattern” and be treated by the same TCMs (Jiang, 2005). As a kidney tonic herb, CT is widely used in OP and AD treatment. Modern studies have provided some compact evidence that CT has positive pharmacologic actions on the skeleton and nervous system. However, it still needs more detailed studies to reveal the mechanisms of CT.

In the present study, for a clear understanding of the effects of CT on OP and AD, a network pharmacology approach was set up to predict possible active ingredients and analyze related pathways. It’s different from previous network pharmacology study on CT (Liu et al., 2017). The “one drug - two diseases” molecular network was conducted for the first time, instead of only focus on one disease. On the one hand, integrated network analysis discovered total 22 active compounds of CT with dual-effects for treating both OP and AD. On the other hand, the patterns of two diseases provided supports for revealing their links. Classified analysis showed that these active compounds may have synergistic effects on many biological function modules and PhGs, flavonoids, terpene, and sterol showed better efficacies. To verify the feasibility and suitability of this conducted network, zebrafish was used to construct OP and AD model in vivo and evaluated the efficacy of four compounds. And putative targets validation was applied to reveal their potential synergies. This combined studies in silico and in vivo provided a new starting point on revealing protective effect of CT on two diseases. It may provide new clues to the correlation between OP and AD pathogenesis, as well as help for the future development of

therapeutic strategies for two disease. Nonetheless, the method still needs improvement and perfection to entirely explore synergetic mechanisms of CT for treating OP and AD. In this study, only certain compounds were selected to validation. It's necessary to further verify other 18 active constituents with underlying targets and pathways by experiments. And the commonalities between OP and AD still need to be further explored and discovered, especially from the perspective of treatment.

In our study, BSS, GE, AA and QU were proved to have protective effects on OP and AD in zebrafish. More delightfully, these valuable constituents also have been experimentally validated in other literature and showed pharmacological activities consistent with that in this paper (Ayaz et al., 2017; Chauhan et al., 2018; King et al., 2015; Ramnath et al., 2018; Thummuri et al., 2018; Vargas-Restrepo et al., 2018; Wang et al., 2019; Yuan et al., 2018). It further proved the effectiveness and rationality of this network, and indicated the dual-effects of the remaining 18 compounds. As for putative targets validation, 9 effective targets consist of TP53, JUN, TNF, IL1B, MAPK14, MAPK3, FGFR1, BMP2, and TGFBR1 were screened as common targets of OP and AD finally. TP53 is a key tumor suppressor, and its activation could induce neuronal apoptosis (Xiao et al., 2019). TP 53, JUN, and SP1 are active transcriptional factors in primary OP (Xie et al., 2015). TNF and IL1B are common inflammatory cytokines with functions of promoting osteoclastogenesis (Geissler et al., 2018) and bone loss (Sang et al., 2017). Furthermore, they both are therapeutic targets for AD through the inhibition of neuroinflammation to protect neurons (Liu et al., 2017). TGFB1, TGFB2, TGFBR1, and TGFBR1 have complex

effects on neuronal inflammation (Lippa et al., 1998) and osteolysiss (Quinn et al., 2001). Bone morphogenetic proteins (BMPs) are one of the factors involved in glial differentiation of neural progenitor cells (Kwak et al., 2014). The upregulated expression of BMP2 has been demonstrated to serve an essential role in osteoblast differentiation (Li et al., 2017). In addition to these experimentally validated targets, the 81 common targets listed in the Table S2 were also expected to be therapeutic targets, but have not been researched or have had preliminary studies in other researches.

It is particularly noteworthy that these valuable targets all related to MAPK and TGF-beta signaling pathways basing on the KEGG enrichment analysis. MAPK signaling pathway regulates cell proliferation, differentiation, survival or apoptosis, inflammation, and innate immunity. It has been reported that the compromised MAPK signaling pathway contributed to the pathology of neurodegeneration such as AD (Kim and Choi, 2015) as well as inhibiting osteoblasts directly (Xiao et al., 2019). As for TGF-β family members, they played different roles in the skeleton with direct effects on bone impairment (Sun et al., 2016), whereas the activation of neuronal TGF-beta signaling increases neurodegenerative disorders and AD-like disease (Tesseur et al., 2006). Thus, MAPK and TGF-beta signaling pathways may be expected to become shared mechanisms for revealing the pathogenesis of OP and AD or slowing the progressions. Besides the two pathways, the 22 active compounds regulated a total of 66 pathways, especially the pathways with the highest p-value, such as Prolactin signaling pathway, FoxO signaling pathway, and Th17 cell

differentiation, will also be worthy of attention and research and as the key to uncovering the correlation between OP and AD. Finally, the discoveries summarized may imply the link between the two diseases in the immune system and the endocrine system.

5. Conclusion

In this work, we proposed a network pharmacology approach, combining PCA analysis，DL screening, multiple targets collection and prediction, PPI network construction， as well as GO and KEGG pathway analysis to probe the efficiency of CT for the treatment of OP and AD. Our results suggested that the 22 active ingredients of CT might mainly regulated signal transduction, endocrine system, immune system, cell growth and death to play an important role in the treatment of OP and AD. To make a better understanding of the mechanisms of CT, this network was deeply excavated and analyzed depending on the type of compounds. In the end, we applied zebrafish OP and AD models separately to identify 4 valuable compounds and related targets, providing a feasible method to connect genome with pharmacodynamics and find dual-effects compounds.

Supplementary information

Table S1. Primer sequences used in quantitative Real-time PCR.

Table S2. The targets list of 81 potential common targets.

Table S3. The active compounds of CT.

Table S4. AD zebrafish model DRR (%) and RE (%).

Author’s contributions

Ying-Qi Li and Yi Chen designed the experiments. Ying-Qi Li analyzed and interpreted the results and wrote the manuscript. Ying-Qi Li, Yi Chen, and Si-Qi Jiang performed the experiments in this study. Jia-Yi Fang checked the data. Fei Li and Ping Li checked the final manuscript. All authors have read and approved the final version of this manuscript.

Competing Interests

None of the authors have any competing interests in the manuscript. And this manuscript/data has not been submitted or published elsewhere for publication.

Acknowledgement

This study was supported by grants from the National Natural Science Foundation of China (No. 81860773, and No. 81873185), Natural Science Foundation of Jiangsu province (No. BK20181327), Xinjiang Science Fund for Distinguished Young Scholar Project (No. 2018Q003).

Abbreviations

OP: osteoporosis; AD: Alzheimer's disease; TCMs: Traditional Chinese Medicines; CT: Cistanche tubulosa (Schenk) Wight; GE: genistein; QU: quercetin; AA: abietic acid; BSS: β-sitosterol; Pre: Prednisolone; Ed: Etidronate Disodium; DPZ: Donepezil HCL; ALP: alkaline phosphatase; TRAP: tartrate resistant acid phosphatase; AChE: acetylcholinesterase; ChAT: choline acetyltransferase; ELISA: enzyme-linked immunosorbent assay; TCMSP: Traditional Chinese Medicine Systems Pharmacology Database and Analysis Platform; PCA: principal component analysis; MV: molecular weight; AlogP: partition coefficient between octanol and water; Hdon: Hydrogen

Donor Count; Hacc: Hydrogen Acceptor Count; DL: drug-likeness; PPI: protein-protein interaction; CPDB: ConsensusPathDB-human; KEGG: Kyoto Encyclopedia of Genes and Genomes; GO: Gene Ontology; AS: average speed; ΔS: speed change; DRR: dyskinesia recovery rate; RE: response efficiency; ALB: albumin; INS: insulin; IL6: interleukin 6; TNF: TNF-alpha; EGF: epidermal growth factor; BMPs: Bone morphogenetic proteins.

References

Abraham A, Cohen A, Shane E, 2013. Premenopausal bone health: osteoporosis in premenopausal women. Clin Obstet Gynecol 56, 722-9.

Ayaz M, Junaid M, Ullah F, et al., 2017. Anti-Alzheimer's Studies on beta-Sitosterol Isolated from Polygonum hydropiper L. Front Pharmacol 8, 697.

Bergen DJM, Kague E, Hammond CL, 2019. Zebrafish as an Emerging Model for Osteoporosis: A Primary Testing Platform for Screening New Osteo-Active Compounds. Front Endocrinol (Lausanne) 10, 6.

Bondi MW, Edmonds EC, Salmon DP, 2017. Alzheimer's Disease: Past, Present, and Future. J Int Neuropsychol Soc 23, 818-31.

Brown C, 2017. Osteoporosis: Staying strong. Nature 550, S15-S7.

Chauhan S, Sharma A, Upadhyay NK, Singh G, Lal UR, Goyal R, 2018. In-vitro osteoblast proliferation and in-vivo anti-osteoporotic activity of Bombax ceiba with quantification of Lupeol, gallic acid and beta-sitosterol by HPTLC and HPLC. BMC Complement Altern Med 18, 233.

Chen Y, Chen PD, Bao BH, et al., 2018. Anti-thrombotic and pro-angiogenic effects

of Rubia cordifolia extract in zebrafish. Journal of Ethnopharmacology 219, 152-60.

Daina A, Michielin O, Zoete V, 2019. SwissTargetPrediction: updated data and new features for efficient prediction of protein targets of small molecules. Nucleic Acids Res 47, W357-W64.

Dengler-Crish CM, Elefteriou F, 2019. Shared mechanisms: osteoporosis and Alzheimer's disease? Aging (Albany NY) 11, 1317-8.

Erkkinen MG, Kim MO, Geschwind MD, 2018. Clinical Neurology and Epidemiology of the Major Neurodegenerative Diseases. Cold Spring Harbor Perspectives in Biology 10.

Franic D, Verdenik I, 2018. Risk Factors for Osteoporosis in Postmenopausal Women - from The Point of View of Primary Care Gynecologist. Zdr Varst 57, 33-8.

Fu ZF, Fan X, Wang XY, Gao XM, 2018. Cistanches Herba: An overview of its chemistry, pharmacology, and pharmacokinetics property. Journal of Ethnopharmacology 219, 233-47.

Geissler S, Textor M, Stumpp S, et al., 2018. Loss of murine Gfi1 causes neutropenia and induces osteoporosis depending on the pathogen load and systemic inflammation. Plos One 13, e0198510.

Huang Y, Mucke L, 2012. Alzheimer mechanisms and therapeutic strategies. Cell 148, 1204-22.

Jiang WY, 2005. Therapeutic wisdom in traditional Chinese medicine: a perspective from modern science. Trends Pharmacol Sci 26, 558-63.

Liu J, Zhu J, Xue J, et al., 2017. In *silico*-based screen synergistic drug combinations

from herb medicines: a case using *Cistanche tubulosa*. Scientific Report 7, 16364.

Jonsson E, Hansson-Hedblom A, Ljunggren O, et al., 2018. A health economic simulation model for the clinical management of osteoporosis. Osteoporosis International 29, 545-55.

Kamburov A, Stelzl U, Lehrach H, Herwig R, 2013. The ConsensusPathDB interaction database: 2013 update. Nucleic Acids Res 41, D793-800.

Kim EK, Choi EJ, 2015. Compromised MAPK signaling in human diseases: an update. Arch Toxicol 89, 867-82.

King TJ, Shandala T, Lee AM, et al., 2015. Potential Effects of Phytoestrogen Genistein in Modulating Acute Methotrexate Chemotherapy-Induced Osteoclastogenesis and Bone Damage in Rats. Int J Mol Sci 16, 18293-311.

Koedijk JB, Van Rijswijk J, Oranje WA, et al., 2017. Sedentary behaviour and bone health in children, adolescents and young adults: a systematic review-supplementary presentation. Osteoporos Int 28, 3075-6.

Kwak YD, Hendrix BJ, Sugaya K, 2014. Secreted type of amyloid precursor protein induces glial differentiation by stimulating the BMP/Smad signaling pathway. Biochem Biophys Res Commun 447, 394-9.

Li F, Yang X, Yang Y, et al., 2013. Antiosteoporotic activity of echinacoside in ovariectomized rats. Phytomedicine 20, 549-57.

Li FM, Li QH, Huang XQ, et al., 2017. Psoralen stimulates osteoblast proliferation through the activation of nuclear factor-kappa B-mitogen-activated protein kinase signaling. Experimental and Therapeutic Medicine 14, 2385-91.

Li S, Yang B, Teguh D, Zhou L, Xu J, Rong L, 2016. Amyloid beta Peptide Enhances RANKL-Induced Osteoclast Activation through NF-kappaB, ERK, and Calcium Oscillation Signaling. Int J Mol Sci 17.

Li TM, Huang HC, Su CM, et al., 2012. Cistanche deserticola extract increases bone formation in osteoblasts. J Pharm Pharmacol 64, 897-907.

Lipinski CA, 2003. Chris Lipinski discusses life and chemistry after the Rule of Five. Drug Discov Today 8, 12-6.

Lippa CF, Flanders KC, Kim ES, Croul S, 1998. TGF-beta receptors-I and -II immunoexpression in Alzheimer's disease: a comparison with aging and progressive supranuclear palsy. Neurobiol Aging 19, 527-33.

Liu C, Guan H, Cai C, Li F, Xiao J, 2017. Lipoxin A4 suppresses osteoclastogenesis in RAW264.7 cells and prevents ovariectomy-induced bone loss. Exp Cell Res 352, 293-303.

Newman M, Ebrahimie E, Lardelli M, 2014. Using the zebrafish model for Alzheimer's disease research. Frontiers in Genetics 5.

Pan H, Zhang J, Wang Y, et al., 2019. Linarin improves the dyskinesia recovery in Alzheimer's disease zebrafish by inhibiting the acetylcholinesterase activity. Life Sci 222, 112-6.

Pan JX, Tang F, Xiong F, et al., 2018. APP promotes osteoblast survival and bone formation by regulating mitochondrial function and preventing oxidative stress. Cell Death Dis 9, 1077.

Parnetti L, Chipi E, Salvadori N, D'andrea K, Eusebi P, 2019. Prevalence and risk of

progression of preclinical Alzheimer's disease stages: a systematic review and meta-analysis. Alzheimers Res Ther 11, 7.

Patel M, 2017. Alzheimer disease: Revising the risk of Alzheimer disease in women. Nat Rev Neurol 13, 575.

Pathan M, Keerthikumar S, Ang CS, et al., 2015. FunRich: An open access standalone functional enrichment and interaction network analysis tool. Proteomics 15, 2597-601.

Pinero J, Bravo A, Queralt-Rosinach N, et al., 2017. DisGeNET: a comprehensive platform integrating information on human disease-associated genes and variants. Nucleic Acids Res 45, D833-D9.

Quinn JM, Itoh K, Udagawa N, et al., 2001. Transforming growth factor beta affects osteoclast differentiation via direct and indirect actions. J Bone Miner Res 16, 1787-94.

Ramnath MG, Thirugnanasampandan R, Nagasundaram N, Bhuvaneswari G, 2018. Molecular Docking and Dynamic Simulation Studies of Terpenoids of I. wightii (Bentham) H. Hara against Acetylcholinesterase and Histone Deacetylase3 Receptors. Curr Comput Aided Drug Des 14, 234-45.

Rizzoli R, 2018. Postmenopausal osteoporosis: Assessment and management. Best Pract Res Clin Endocrinol Metab 32, 739-57.

Ru J, Li P, Wang J, et al., 2014. TCMSP: a database of systems pharmacology for drug discovery from herbal medicines. J Cheminform 6, 13.

Safran M, Dalah I, Alexander J, et al., 2010. GeneCards Version 3: the human gene

integrator. Database-the Journal of Biological Databases and Curation.

Sang C, Zhang J, Zhang Y, Chen F, Cao X, Guo L, 2017. TNF-alpha promotes osteoclastogenesis through JNK signaling-dependent induction of Semaphorin3D expression in estrogen-deficiency induced osteoporosis. J Cell Physiol 232, 3396-408.

Sofi F, Valecchi D, Bacci D, et al., 2011. Physical activity and risk of cognitive decline: a meta-analysis of prospective studies. J Intern Med 269, 107-17.

Sucher NJ, 2013. The application of Chinese medicine to novel drug discovery. Expert Opin Drug Discov 8, 21-34.

Sun X, Liu J, Zhuang C, et al., 2016. Aluminum trichloride induces bone impairment through TGF-beta1/Smad signaling pathway. Toxicology 371, 49-57.

Szklarczyk D, Morris JH, Cook H, et al., 2017. The STRING database in 2017: quality-controlled protein-protein association networks, made broadly accessible. Nucleic Acids Res 45, D362-D8.

Tao W, Xu X, Wang X, et al., 2013. Network pharmacology-based prediction of the active ingredients and potential targets of Chinese herbal Radix Curcumae formula for application to cardiovascular disease. Journal of Ethnopharmacology 145, 1-10.

Tesseur I, Zou K, Esposito L, et al., 2006. Deficiency in neuronal TGF-beta signaling promotes neurodegeneration and Alzheimer's pathology. J Clin Invest 116, 3060-9.

Thummuri D, Guntuku L, Challa VS, Ramavat RN, Naidu VGM, 2018. Abietic acid attenuates RANKL induced osteoclastogenesis and inflammation associated osteolysis by inhibiting the NF-KB and MAPK signaling. J Cell Physiol 234, 443-53.

Vargas-Restrepo F, Sabogal-Guaqueta AM, Cardona-Gomez GP, 2018. Quercetin

ameliorates inflammation in CA1 hippocampal region in aged triple transgenic Alzheimer s disease mice model. Biomedica 38, 69-76.

Vieira MNN, Lima RaS, De Felice FG, 2018. Connecting Alzheimer's disease to diabetes: Underlying mechanisms and potential therapeutic targets. Neuropharmacology 136, 160-71.

Wang YX, Xia ZH, Jiang X, et al., 2019. Genistein Inhibits Abeta25-35-Induced Neuronal Death with Changes in the Electrophysiological Properties of Voltage-Gated Sodium and Potassium Channels. Cell Mol Neurobiol 39, 809-22.

Wenhai H, Li. C, Shen. Z, Zhu. X, Xia. B, Li. C, 2016. Development of a Zebrafish Model for Rapid Drug Screening against Alzheimer’s Disease. Journal of Pharmacy and Pharmacology 4, 174-85.

Wu CR, Lin HC, Su MH, 2014. Reversal by aqueous extracts of Cistanche tubulosa from behavioral deficits in Alzheimer's disease-like rat model: relevance for amyloid deposition and central neurotransmitter function. BMC Complement Altern Med 14, 202.

Xia JW, Zhong Y, Huang GZ, Chen YJ, Shi HP, Zhang ZL, 2012. The relationship between insulin resistance and osteoporosis in elderly male type 2 diabetes mellitus and diabetic nephropathy. Annales D Endocrinologie 73, 546-51.

Xiao H, Qin X, Wan J, Li R, 2019. Pharmacological Targets and the Biological Mechanisms of Formononetin for Alzheimer's Disease: A Network Analysis. Med Sci Monit 25, 4273-7.

Xie W, Ji L, Zhao T, Gao P, 2015. Identification of transcriptional factors and key

genes in primary osteoporosis by DNA microarray. Med Sci Monit 21, 1333-44.

Yuan Z, Min J, Zhao Y, et al., 2018. Quercetin rescued TNF-alpha-induced impairments in bone marrow-derived mesenchymal stem cell osteogenesis and improved osteoporosis in rats. Am J Transl Res 10, 4313-21.

Zhang W, Huang J, Wang W, et al., 2016. Extraction, purification, characterization and antioxidant activities of polysaccharides from Cistanche tubulosa. Int J Biol Macromol 93, 448-58.

Zhong G, Wang Y, Zhang Y, Guo JJ, Zhao Y, 2015. Smoking Is Associated with an Increased Risk of Dementia: A Meta-Analysis of Prospective Cohort Studies with Investigation of Potential Effect Modifiers (vol 10, e0118333, 2015). Plos One 10.